Chapter 3:

Label-Free Fluorometric Detection of Adulterant Malachite Green Using Carbon Dots Derived from the Medicinal Plant Source *Ocimum tenuiflorum*

3.1 Introduction

3.1.1 Malachite Green: A Common Food Adulterant with Harmful Effects

Food adulteration is an emerging problem in developing countries adversely affecting human health and environment. Malachite green is well-known triarylmethane dye commonly used in the textile, aquaculture, fungal staining, health and paper industries. It is known to cause many harmful and genotoxic effects. Inside the body, it can cause mutagenesis, respiratory failure, cancer, organ damage to spleen, liver, kidney, thyroid, heart and sex organs.[1,2] Inspite of being banned in most developed countries and not approved by US Food and Drug Administration, its use is prevalent in many countries due to meagre cost, easy synthesis and availability. Malachite green is persistent in the environment and severely toxic to a wide variety of aquatic and terrestrial animals.[2] Regardless of these detrimental effects, its use is still prevalent in developing countries. Poor farmers use these chemical dyes to colour green vegetables to give them a greener and fresher appearance. These dyes are not easily removable even after washing and eventually end up in the body.

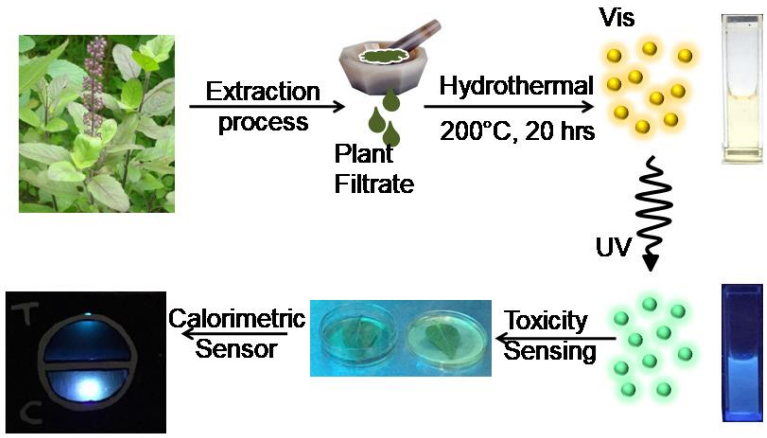

Figure 3.1: Schematic illustration of synthesis of carbon quantum dots using *Tulsi* as precursor and their application in sensing malachite green by strong quenching of their fluorescence

3.1.2 Detection of Malachite Green

Many techniques have been reported for the sensitive detection of malachite green using SERS,[3] HPLC,[4] mass spectrometry,[5] ELISA,[6,7] magnetic molecularly imprinted polymers(MMIPs)[8] and aptamer-based approaches.[9] However, these techniques require expensive and sophisticated instruments which may not always be a sustainable method of ultrafast detection in developing countries. Recently, fluorescence spectroscopy-based techniques have emerged as a very popular method of detection for many molecules because of their high sensitivity, rapid detection and analysis. Malachite green itself shows strange fluorescence behaviour. It has negligible fluorescence in aqueous environment but its fluorescence gets enhanced many fold when it binds to certain nucleic acids. This principle has been used to develop an aptamer-based sensor for the detection of adenosine using the fluorescence of MG.[10] Studies have been done on understanding the relaxation kinetics of S2 fluorescence in MG using femtosecond fluorescence spectroscopy.[11] The interaction of malachite green with many molecules, such as lysozyme,[12] has also been investigated using fluorescence spectroscopy. In the past years, many efforts to detect

malachite green have been made using fluorescence-based methods.[4] Although these methods might hold some advantages like fast sensitive detection and simple treatment, they are not very cost effective for routine analysis.

3.1.3 Use of Fluorescent Probes for Detection of Analyte

In this method the choice of the fluorescent probes is crucial for rapid and sensitive detection of molecules. Traditionally used organic fluorescent dyes require sophisticated synthetic procedure, narrow excitation spectra, small Stokes shifts and suffer from rapid photobleaching. Some of these drawbacks can be overcome with the use of inorganic quantum dots. However, the use of inorganic quantum dots is rather limited due to their low aqueous solubility, chemical reactivity, high cytotoxicity and poor biocompatibility.[13] Researchers are now exploring the use of carbon quantum dots as fluorescent probes, an alternative to inorganic quantum dots.

3.1.4 Carbon Quantum Dots as Fluorescent Probes

Carbon quantum dots have gained huge attention in the recent years due to their fascinating and versatile nature with respect to their diverse and flexible precursor sources and intrinsic robustness in performance capabilities.[13] They have several advantages over their other organic and inorganic metal counterparts like ease of production, low toxicity, low cost of production, water solubility, wavelength tunable emission, good photostability, facile functionalization, chemical inertness and biocompatibility.[14,15] They have been used in a wide range of applications like efficient battery devices, anticounterfeiting, LED systems, bioimaging, toxicity sensing, drug delivery, theranostics and cancer targeting.[16–20] Owing to their interesting optical and photoluminescence properties, carbon quantum dots have been used extensively for detection of chemicals.[20,21] They hold a great potential in

practical and easy detection of malachite green used as a food adulterant in developing countries. An effort to design a sustainable and affordable sensor is warranted for detecting this toxic dye. Carbon quantum dots can be a great candidate for this purpose by utilizing their intrinsic fluorescence property.

3.1.5 Methods of Synthesis of CQDs

Carbon quantum dots can be synthesized through either top-down or bottom-up approach employing multiple methods such as arc discharge,[22] laser ablation,[23] thermal,[24] ultrasonic,[25] microwave-assisted synthesis,[26] electrochemical exfoliation,[27] acidic oxidation,[28] solvothermal[29] and hydrothermal synthesis.[30] Some of these methods enhance the fluorescence by employing heteroatom doping and surface passivation steps. Among these, hydrothermal method has been extensively used as a cheaper eco-friendly alternative which often uses natural sources as precursors eliminating the need of surface passivation of the carbon dots. A huge variety of natural sources have been used like apple, cashew and many others.[31–45] This synthetic route has garnered great interest because of the simplicity of the synthesis approach eliminating the need of using costly and sophisticated procedures, additional and often toxic chemical reagents, solvents and acids.

3.1.6 Choice of Carbon Precursor for CQD Synthesis: *Ocimum tenuiflorum* or Tulsi

Ocimum tenuiflorum (or Tulsi), is a well-known medicinal plant belonging to the family *Lamiaceae* which has been used for centuries in Ayurvedic and herbal formulations. Known as “Queen of herbs”, it possesses many essential oils having many therapeutic effects in the body. It contains many antioxidant and phenolic compounds like cirsilineol, circimaritin, isothymusin, apigenin and rosameric acid and eugenol. It also contains carvacrol and sesquiterpine hydrocarbon caryophyllene. Two

flavanoids, orientin and vicenin also exist in the plant extract.[46] Tulsi is known to have numerous healing properties in the body like curing cough, cold, headache, influenza, fever, colic pain, asthma, hepatic diseases, flatulence, migraine headache, skin diseases, arthritis and wounds. It is known to promote longevity, has antibacterial and anticancer properties and is used as an antidote for many toxins. It boosts the immune system preventing viral, bacterial, protozoan and fungal infections.[46] It is interesting to see if carbon quantum dots synthesized using *Tulsi* as precursor, can emulate the innate properties of the plant and their effect on antibacterial, antifungal and antioxidant activities. Carbon dots using *Tulsi* have been previously reported for sensing Pb^{2+} ions.[47]

In the present work, we have synthesized carbon quantum dots using a green eco-friendly and medicinal source through hydrothermal method in a facile one-step approach. This method is advantageous as there is no requirement of extensive procedures and costly or toxic materials. The as synthesized carbon quantum dots were characterized and found to exhibit a monodisperse size distribution and amorphous nature. Various physicochemical and optical properties were also characterized. Blue fluorescence is observed on excitation at λ_{ex} = 320 nm under a UV source. The carbon dots were used for the detection of malachite green, a common toxic adulterant in developing countries through fluorescence quenching based method. This is a simple, rapid, label-free and cost effective method of detection and can easily be accessible in developing countries. Real aquaculture water and vegetable samples have also been used to test the practical efficacy and feasibility of this detection method. It was observed that this method proved to be highly sensitive for MG detection and could detect levels as low as 18 nM. A very simple calorimetric sensor is designed to detect MG which can be used in common households. Further,

these carbon quantum dots have also been tested for checking their antibacterial, antifungal and antioxidant properties. A very appreciable antioxidant activity is seen whereas cytotoxicity is seen to very low making them suitable for biological applications.

3.2 Results and Discussions

Carbon quantum dots were synthesized using indigenous *Tulsi* as the precursor material by hydrothermal method at 200°C for 12 hours converting organic compounds in the plant to carbon dots. Further, these carbon dots were characterised using DLS, TEM, Raman, FTIR, XPS, UV-Vis and fluorescence spectroscopy. They were used to detect a carcinogenic compound, malachite green and were tested for antibacterial, antifungal and antioxidant activity.

3.2.1 Morphology and Surface Properties of Carbon Quantum Dots

TEM was used to estimate the size and morphology of carbon dots. The carbon dots were uniformly monodispersed in solution and were seen to possess a quasispherical shape with an average size ranging from 1 nm to 3 nm within a narrow distribution range (Figure 3.2A&B). The SAED pattern shows diffused concentric rings suggesting the presence of amorphous carbon. Hydrodynamic diameter of the carbon dots was measured around 3 nm (Figure 3.2C) using DLS. To further understand the surface potential of the prepared carbon dots, zeta potential was investigated. The measured zeta potential was negative, 18 mV (Figure 3.2D), which indicates electro negative surface charge at the interfacial double layer.[25] Carbon dots are considerably stable owing to the electrostatic repulsion between the carbon dots due to the presence of net negative charge. This is commonly found in many synthesized carbon dots.[48–50]

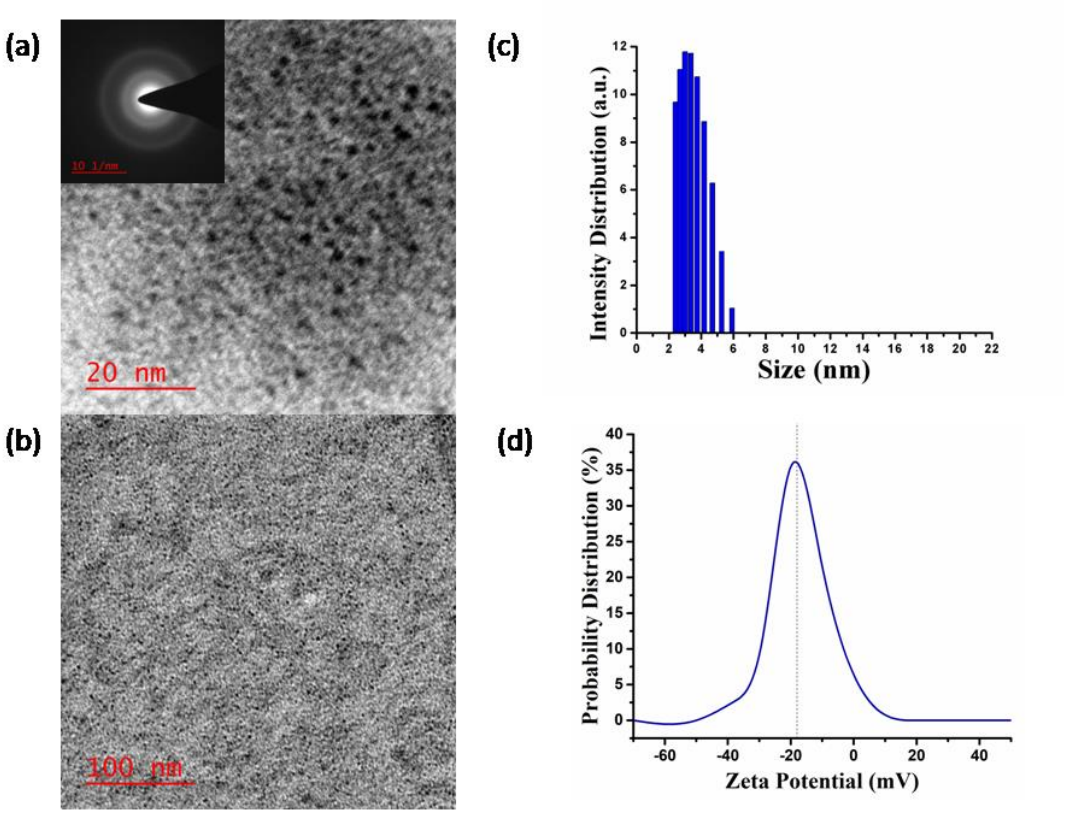

Figure 3.2: Morphology and Structure of carbon quantum dots. TEM images of carbon quantum dots at (A) 20 nm resolution. The inset shows the SAED pattern of the carbon dots (B) at 100 nm resolution (C) size distribution of carbon quantum dots by Dynamic Light Scattering (D) zeta potential of carbon quantum dots

3.2.2 Elucidation of Surface Functional Groups of CQDs through FTIR and XPS

XPS and FTIR studies were conducted to gain insight into the structural composition and functional groups on the surface of quantum dots. The XPS survey spectrum revealed the presence of prominent C1s, O1s and N1s peaks at 285, 400 and 531 eV (Figure 3.3A). The C1s core level was deconvoluted to into four components corresponding to C-C (283.6 eV), C=C (284.3 eV), C-N (285.1 eV), C-O (286.9 eV) respectively (Figure 3.3B). The data shows the percentage distribution of carbon species present on the surface of the carbon quantum dots having maximum distribution for C-C/C-H bonds in the sp^3 hybridisation state compared to sp^2 hybridised C=C bonds having 9.14% area distribution. Moreover, it can be seen that

the quantum dot surface is rich in both nitrogen and oxygen containing functional groups having 25.29% and 20.54% area distribution respectively.

Table 3.1: The presence of C-N ,C-H and C=C is consistent with FTIR data of the same sample. The resolution of the XPS system used for the measurement is 0.1 eV. Instrument make - Kratos Axis Ultra DLD.1486.4 eV Al k alpha line is used for measurement.

Peak Position	FWHM	% Area	Chemical Species
283.6[1]	1.22	45.03	C-C/C-H
284.3[1]	1.02	9.14	Sp^2 Carbon (C=C)
285.1[1]	1.29	25.29	C-N
286.9[2]	1.86	20.54	C-O

FTIR spectrum is consistent and supports the result by showing prominence of both sp^2 and sp^3 hybridized carbon containing functional groups mainly in conjugation with nitrogen and oxygen (Figure 3.3C). A broad peak at 3350 cm^{-1} is caused mainly by phenolic stretch (OH) and partial contribution of amine stretch (NH) resulting in higher polarity and hydrophilicity of the samples. Two small peaks at 2975 and 2931 cm^{-1} are attributed to the alkyl stretch caused by sp^2 and sp^3 hybridised carbon. Peaks at 2361 cm^{-1} and 2334 cm^{-1} may be caused by triple bonded carbon-carbon and carbon-nitrogen nitrile groups. The peaks ranging from 1700–1500 cm^{-1} are assigned to aldehyde/ketonic stretch (C=O), C=C double bond and N-H bending which can also be present because of amide stretch. The sharp peak at 1400 cm^{-1} is caused by C-H scissoring while the peak at 1075 cm^{-1} is assigned to ether stretch (C-O). Finally, the peaks at 875, 798, 713 and 685 cm^{-1} are ascribed to mainly single, double bonded and aromatic C-H bending. These results indicate that the surface of carbon dots is rich in oxygen and nitrogen containing functional groups thereby ensuring good aqueous solubility.[30,31]

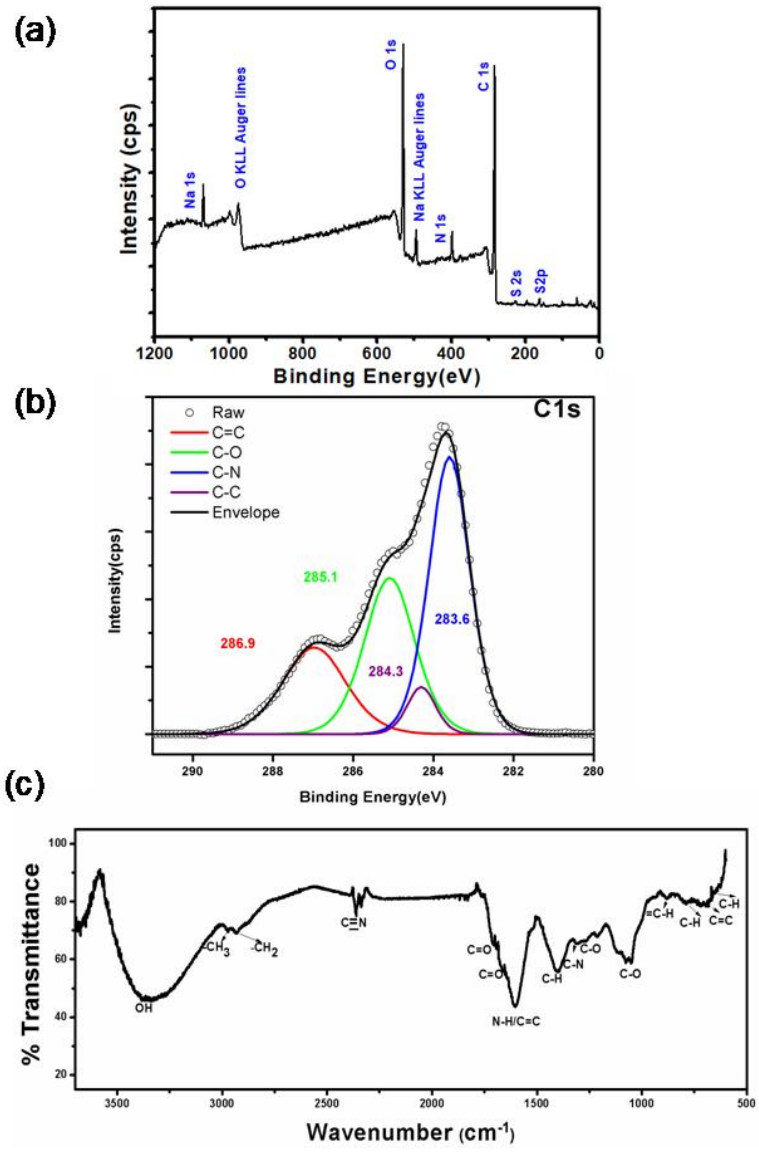

Figure 3.3: Structural analysis (A) Wide range spectra by XPS (B) High resolution XPS spectra of C1s core level (C) FTIR spectra of carbon quantum dots

3.2.3 XRD Profile of CQDs

An X-ray diffraction profile was studied which showed a broad reflection peak centred at around 2θ=24.9° which was in congruence with the (002) plane characteristic of graphitic materials having high sp^3 disorder. Interlayer lattice spacing of 3.34 Å is very slightly larger than 3.33 Å spacing seen in bulk graphite indicating poor crystallization as often found in carbon dots.[51,52] (Figure 3.4). This result is in

agreement with the selected area electron diffraction (SAED) pattern which confirms the amorphous state of the carbon dots. This may be caused by defects created by the abundance of oxygen containing functional groups observed in FTIR and XPS spectra.

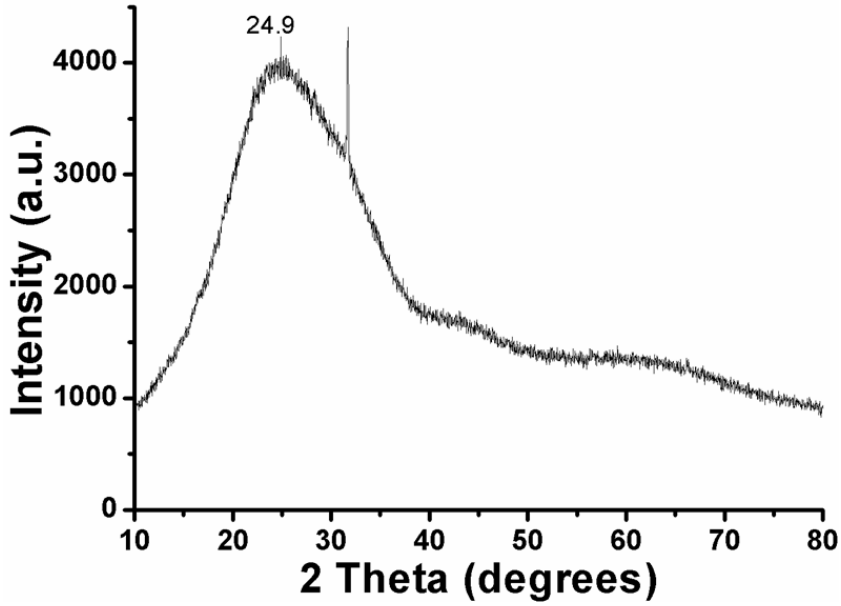

Figure 3.4: XRD pattern of carbon quantum dots

3.2.4 CQD Stability in Various Conditions

The synthesized carbon dots were homogenous for a long duration (3 months) without any noticeable aggregation at 4°C. The fluorescence intensity also did not show significant change after the long-term storage. The observed zeta potential (-18 mV) helps in explaining the hydrophilic colloidal nature which prevents the carbon dots from visible flocculation or aggregation and allows long term storage stability of the solution. To check the stability of carbon quantum dots, ionic strength was increased by adding NaCl (333 μN-4.67 mN). Photoluminescence spectra showed no difference as compared to control confirming the high stability of the synthesized quantum dots [Figure 3.5&3.6]. The abundance of carbonyl, carboxyl and hydroxyl

groups may have contributed to their long term solubility and storage. Hydrothermal reaction modified the organic molecules like carbohydrates, secondary metabolites etc. to these functional moieties on the surface of the carbon dots.

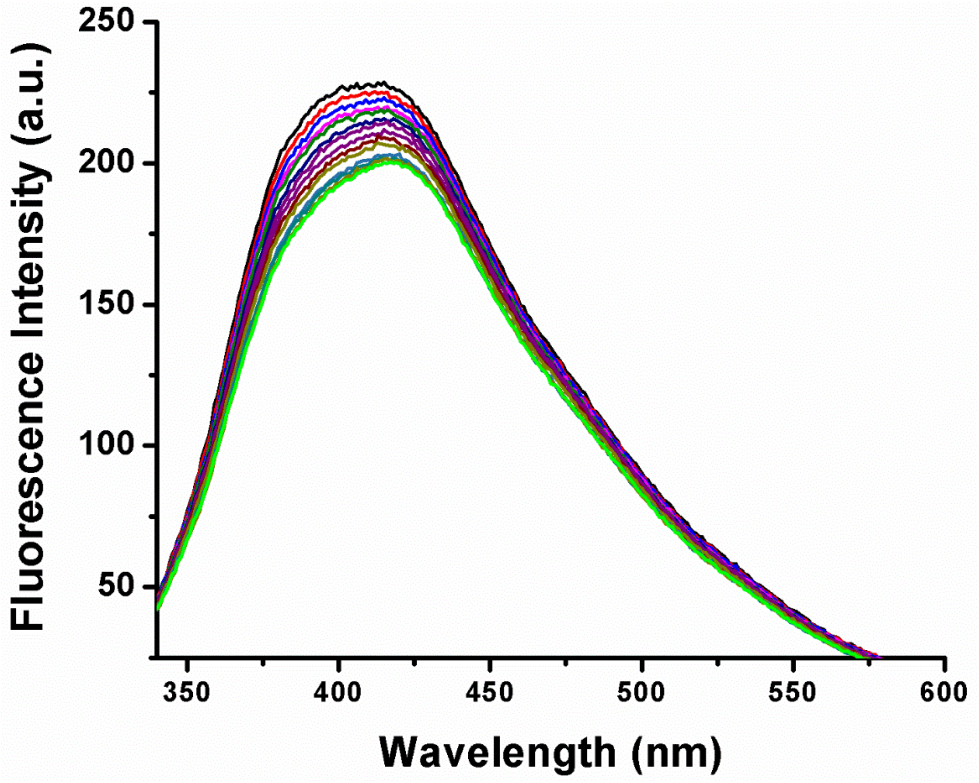

Figure 3.5: Photoluminescence spectra of carbon dots on addition of ultrapure water ranging from 0 to 130 µl

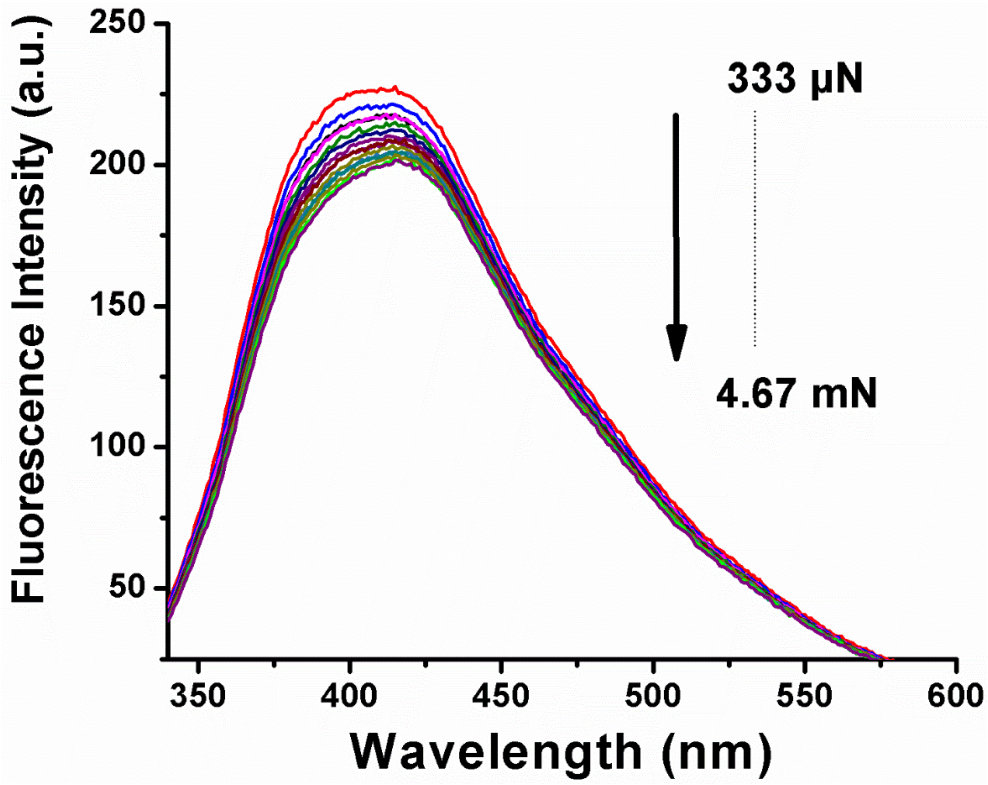

Figure 3.6: Photoluminescence spectra of carbon dots on increasing ionic strength by addition of NaCl (333 µN-4.67 mN)

3.2.5 Optical Properties of Carbon Quantum Dots

The prepared carbon dots appeared yellowish-brown with excellent aqueous solubility. The absorbance spectrum of carbon quantum dots showed maximum absorption in the UV-blue wavelength range extending beyond 500 nm consistent with most carbon dot absorption spectroscopy data[53] (Figure 3.7A). Two peaks at 254 and 315 nm were observed which may be attributed to the π-π* and n-π* electronic transition of C=C/C=N and C=O double bonds.[30,31] Oxygen and nitrogen groups may arise from the surface while carbon-carbon bonds may be present inside the core. One of the most remarkable properties of carbon dots is their intrinsic photoluminescence. It showed characteristic excitation-dependent fluorescence with maximum intensity for 320 nm excitation wavelength (Figure 3.7B). Carbon quantum

dots reflected strong blue fluorescence near 405 nm with a Stokes' shift of 90 nm as seen with other reports.[33]

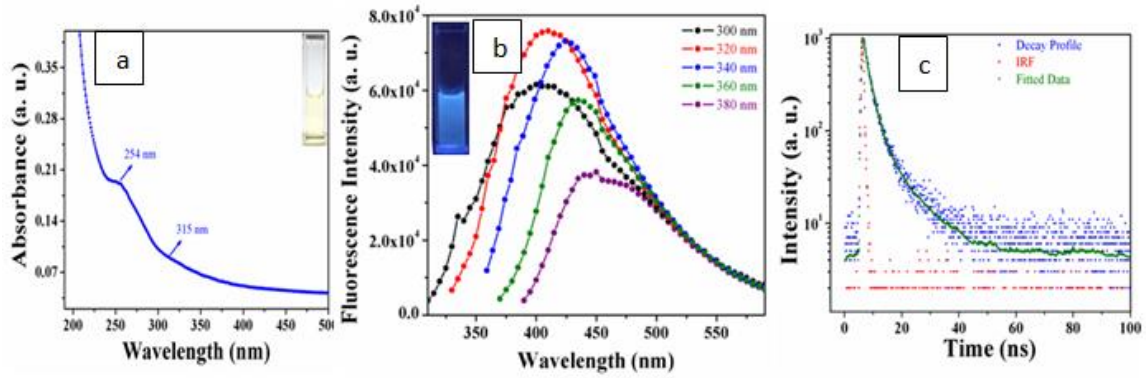

Figure 3.7: Spectroscopic Analysis (A) UV-Vis spectra of carbon quantum dots (B) Photoluminescence spectra of carbon quantum dots excited at 300, 320, 340, 360, 380 nm (C) Time- resolved lifetime decay profile of fluorescent carbon quantum dots showing an average lifetime of τ_{avg} = 2.83 ns

Further, the quantum yield of synthesized carbon dots was found out to be 11.5%, higher than the average quantum yields of carbon dots synthesized from natural sources, reported in literature using quinine sulphate as reference in 0.1 M H_2SO_4.[31–33] Hydroxyl and amide groups may contribute to the efficient enhancement of the intrinsic state emissions in the carbon dots by suppressing the non-radiative electron-hole recombination leading to the increased photoluminescence.

The time-resolved fluorescence decay profile was measured by time-correlation single photon counting method at the emission maximum. The PL decay curve was obtained to analyze the photoluminescence lifetime of carbon dots at room temperature (Figure 3.7C). It fitted very well with a tri-exponential function (adjusted R^2 value = 0.9999) as often found in literature.[50,54] The observed values were found to be τ_1 = 0.81931 ns, τ_2 = 2.4343 ns and τ_3 = 9.74326 ns and the calculated average lifetime was found to be τ_{avg} = 2.83 ns using the following equation-[50]

$$\tau=(A_1\tau_1+A_2\tau_2+A_3\tau_3)/(A_1+A_2+A_3)$$

where A_i represents the contributing fraction of emitting species τ_i = 1,2,3. The observed short lifetime makes these carbon dots very amenable for optoelectronic, biosensor and bioimaging applications. Multiexponential emission decay is typically observed in carbon dots.[21,51] This may be caused by different discrete states,[55] localized electrons in the conduction band in shallow trapped states, rapid band gap transition and emission related to oxygen-containing functional groups. Short nanosecond lifetime may also be indicative of fast radiative recombination of exciton species.[54] Carboxyl groups have electron withdrawing capabilities while hydroxyl groups have an electron donating tendency. Their rapid inter-dynamics might contribute to the short-lived emission with multiple emitting species.[20]

The underlying root for the mechanism of photoluminescence in carbon dots has always been a matter of much debate. Some researchers hypothesize that the radiative recombination of the excitons, or electron-hole pairs localized within sp^2 clusters of carbon aromatic moieties is responsible for the origin of PL while others speculate emissive energy traps as the main contributing factor.[56–58] Other reasons often mentioned are free zig zag edges, quantum confinement and surface defect sites due to functionalization by the presence of many electron-accepting oxygen and nitrogen-rich groups causing band gap like transition both of which are abundant in the carbon quantum dots.[30,31,39,54,59] Some groups have shown the role of solvent effect in affecting PL properties like the excitation-dependent PL behaviour which has also been shown to depend on the surface state of the particular carbon dot.[39,60,61] Another reason shown to affect the origin of PL was the difference in the size of the formed carbon quantum dots.[27,62] Different emissive states have also been shown to be the reason for such fluorescence characteristics.[63]

3.2.6 *In vitro* antioxidative assay of the Synthesized CQDs

The study of free radical scavenging activity of the synthesized carbon dots gives an idea about the activity and association of these carbon dots with biomolecules and metabolites. DPPH assay is the most widely used method for the assessment of radical scavenging activity of a compound or a plant extract. DPPH is a stable nitrogen-centred free radical that shows a characteristic absorption at 517 nm. On increasing concentration of carbon quantum dots, decrease of absorbance peak is observed (Figure 3.8A) and deep violet to light yellow colour change can be visualised owing to reduction of DPPH (Figure 3.8B) showing the excellent antioxidant property of the carbon dots. This illustrated that carbon quantum dots synthesized from *Tulsi* extract showed potent free radical scavenging activity in dose-dependent manner (106.3-531.5 µg/ml). The antioxidants react with DPPH and convert it to 1,1- diphenyl-2-picryl hydrazine. Carbon dots quenched the activity of DPPH by donating electrons. The residual DPPH is quantifiable by comparing absorbance at 517 nm against the blank, and the percent inhibition was calculated (Figure 3.8C). This is consistent with the nature of carbon dots which act as antioxidants by scavenging free radical species.[64]

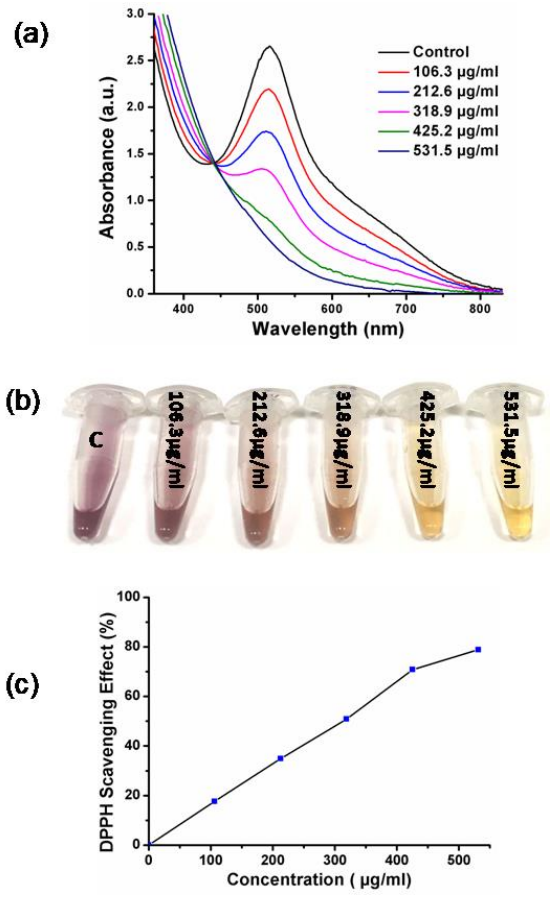

Figure 3.8: Antioxidant Assay (A) UV-Vis Spectra of DPPH radical scavenging activity on addition of carbon quantum dots (B) Different concentrations of carbon quantum dots (106.3-531.5µg/ml)) in DPPH-methanol solution (C) DPPH scavenging effect in percentage for various concentrations of carbon quantum dots (106.3-531.5µg/ml) in DPPH-methanol solution

3.2.7 Cell Viability Bioassay of Carbon Quantum Dots

Carbon quantum dots prepared from *Tulsi* were tested for their potential against bacterial growth to see if the innate antibacterial property of the plant was still conserved or not. Antibacterial activity was tested against four test bacteria, *Pseudomonas aeruginosa* (Gram negative), *Escherichia coli* (Gram negative), *Staphylococcus aureus* (Gram positive) and *Bacillus subtilis* (Gram positive). MTT assay and simple bacterial OD_{600} was assessed together to check the cell viability after treatment of cells with different concentrations of carbon dots (50, 150 and 250 µg/ml). The results showed that the carbon quantum dots were scarcely toxic to the

cells even after 24 hours of incubation time (Figure 3.9A&B). Slight destruction of cells, especially Gram negative strains, may be caused by the obstruction of important receptors and transporters on the cell surface which ship important metabolites by blockage caused by the carbon quantum dots. Similarly, antifungal activity of the synthesized carbon quantum dots was tested against four fungal species-*Candida albicans*, *Aspergillus terreus*, *Colletotrichum falcatum* and *Aspergillus niger* by Agar well diffusion method on Muller Hinton Agar plates in triplicate. No zone of inhibition was observed for different concentrations of carbon quantum dots (1.67, 5 and 8.3 mg/ml) as compared to control (Figure 3.9C-F). These results suggest excellent biocompatibility of the carbon dots in bacterial and fungal cells which can be harnessed for bioimaging and molecular delivery experiments.

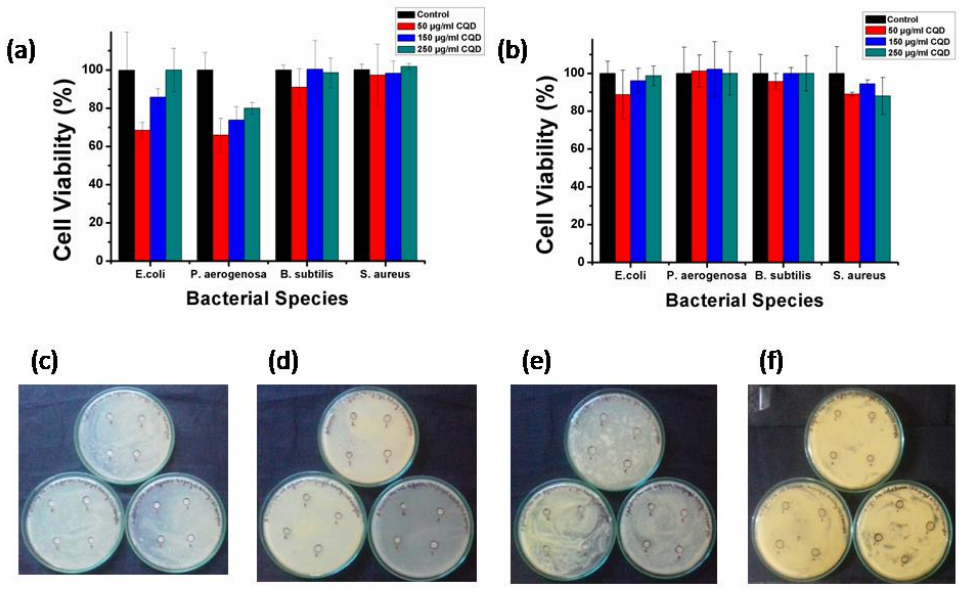

Figure 3.9: Antibacterial and Antifungal Assays. (A) Bacterial cell viability at OD_{570} for MTT assay (B) Bacterial cell viability at OD_{600}. Antifungal Activity on (C) *Candida albicans* (D) *Aspergillus terreus* (E) *Colletotrichum falcatum* (F) *Aspergillus niger*

3.2.8 Toxicological detection strategy for Malachite Green using fluorescence

The heteroatom-rich surface and high quantum yield of *Tulsi*-derived carbon quantum dots, make them easy label-free photoluminescence probes for sensing toxic chemicals. Malachite green is known to possess toxicity and cause carcinogenesis in animal models.[2] Carbon quantum dots have been investigated for easy and efficient detection of malachite green. The sensitivity of carbon dots to malachite green was calibrated by fluorescence titration assay. The photoluminescence of carbon dots is very sensitive to the presence of MG under optimal conditions and decreases drastically with incremental MG concentration (Figure 3.11A). MG itself has very low photo luminescence at the same excitation wavelength (Figure 3.10), but its fluorescence peak gains prominence when added to carbon dots. To investigate if any new species is formed, the UV-Vis spectra was measured with increasing concentration of malachite green at fixed concentration of carbon quantum dots. Neither any peak shift nor any new peak was observed on increasing the concentration of malachite green suggesting no new product was formed (Figure 3.11B).

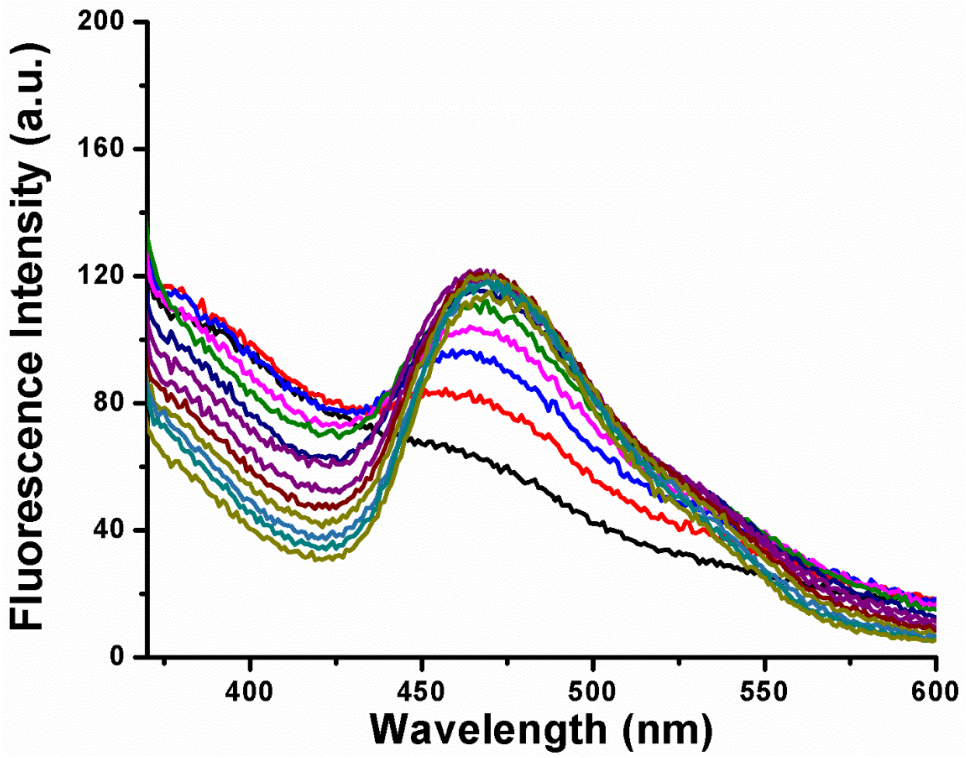

Figure 3.10: Emission spectra of Malachite Green at Ex_{320} with increasing concentration

To predict the possible mechanism of sensing, the fluorescence quenching behaviour is investigated. Fluorescence quenching depending on the type of molecular interactions can be either static or dynamic/collisional. The former involves non-fluorescent complex formation between the quencher and the fluorophore, whereas the latter involves the electron transfer from the excited state fluorophore to ground state quencher.[52] Since physical molecular contact is an imperative condition for both static and dynamic quenching mechanisms, the surface functional groups play an important role in affecting the binding affinity between the quencher and carbon dots thereby affecting its fluorescence intensity. To understand the possible quenching mechanism, the fluorescence quenching behaviour was characterized by fitting the data into the standard linear regression Stern–Volmer equation-[37,49,65]

$$\frac{F_{\circ}}{F} = K_{SV}.C + 1$$

Relative fluorescence response for (F0/F) as a function of MG concentration is shown in Figure 3.11C where, F0 and F are the fluorescence emission intensities of the carbon dots at 405 nm (λ_{ex} = 320 nm) in the absence and presence of malachite green respectively, Ksv is the Stern–Volmer quenching constant and C is the concentration of the quencher (MG). If this plot shows a degree of linearity, it indicates the role of dynamic quenching. If it is non-linear, it attributes the presence of both static and dynamic quenching of fluorescence as the mechanism of interaction.[21] As observed in the Figure 3.11C, the Stern–Volmer plot shows an exponential trend over the range 0–120 nM. This shows involvement of both static and dynamic quenching. For simple calculation, a linear line was fitted over a small range (18.2-63.7 nM). The Stern–Volmer quenching constant (Ksv) was calculated to be 31.2×10^6 mol^{-1} dm^3 with the correlation coefficient R^2 of 0.984. The limit of detection (LOD) was calculated by using the equation $3\sigma/m$ (where σ represents the standard deviation of the blank signal and m is the slope of the plot) and was found to be 18 nM showing excellent capability for the detection of nanomolar quantities of malachite green.

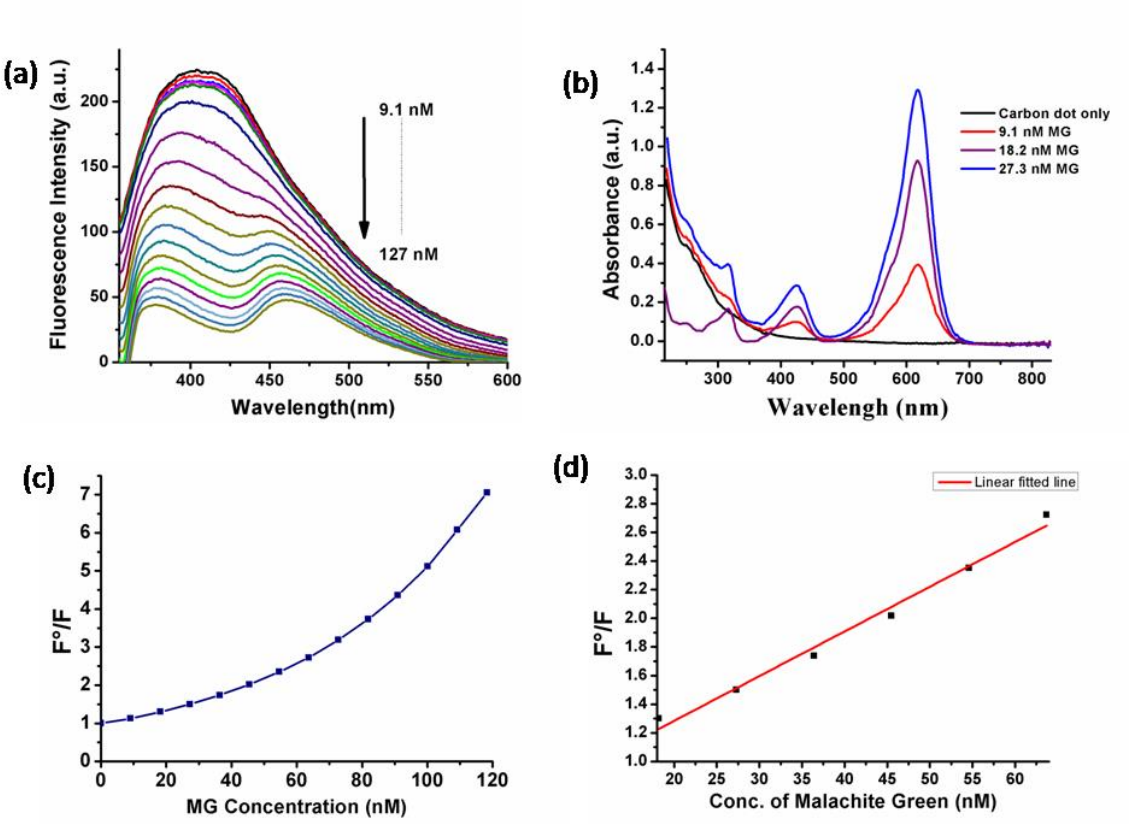

Figure 3.11: Toxicity Sensing of malachite green through quenching of photoluminescence of carbon quantum dots (A) Fluorescence quenching of carbon quantum dots by incremental addition of malachite green (9.1-127 nM) (B) UV-Vis absorption spectra showing no new entity formed complex since no new peak is formed (C) Stern-Volmer Plot for increasing concentrations of malachite green (D) Linear fitted Stern-Volmer Plot for calculation of LOD over a small range (18.2-63.7 nM)

3.2.9 Computational Studies for Understanding the Interaction between the CQD Surface and Malachite Green

In silico studies were performed to understand the interaction between malachite green and carbon quantum dots more deeply. The interaction energy between malachite green and model of carbon quantum dot and functionalised model of carbon quantum dot were calculated separately at M062X/6- 31G(d,p) level of theory in gas phase and also in aqueous media employing SMD solvation model. For carbon dot functionalisation, epoxy (-O-), hydroxyl anion (OH-), cyno (-CN) and

carboxylic (-COOH) groups were added to the optimised model of carbon dots. All optimized geometries of malachite green, model of carbon dots, functionalised model of carbon dots, complex of malachite green with model of carbon dots and complex of malachite green with functionalised models of carbon dots are presented in Figure 3.12. The complex of malachite green with model of carbon dots was found to be lowered in energy by 32.71 kcal/mol in gas phase with respect to their free reactants i.e. sum of energies of malachite green and model of carbon dots. However, in the aqueous medium, the same complex was found to be lowered in energy by only 19.42 kcal/mol. Therefore, in going from gas to aqueous media, the stability of the complex formed between malachite green and model of carbon quantum dots decreases which may arise due to the charge distribution of the complex in aqueous medium since malachite green possesses partial positive charge and also co-planar vibrations are more in water preventing efficient stacking. The interaction energy between malachite green and only carbon side of the functionalised model of carbon quantum dots (Figure 3.12E) was found to be 25.70 kcal/mol in aqueous medium with respect to the free reactants. This suggests increase in the stability of the system because of the presence of functional groups. However, when malachite green interacts with functionalised carbon dots towards the side-containing functionalised sites (Figure 3.12F), the interaction energy is found to be 121.25 kcal/mol. This large increase in interaction energy is due to the electrostatic interactions between negatively charged groups on the carbon dots (hydroxyl, epoxy, carboxyl, cyano) with the partial positive charge on malachite green. There is also possibility of hydrogen bonds between hydrogen bound to oxygen (hydroxyl, carboxyl) in carbon quantum dots with nitrogen in malachite green. Thus, not only functionalisation of carbon dots but also the site of

functionalisation plays a role in increasing the stability of the complex formed between malachite green and functionalised model of carbon dots.

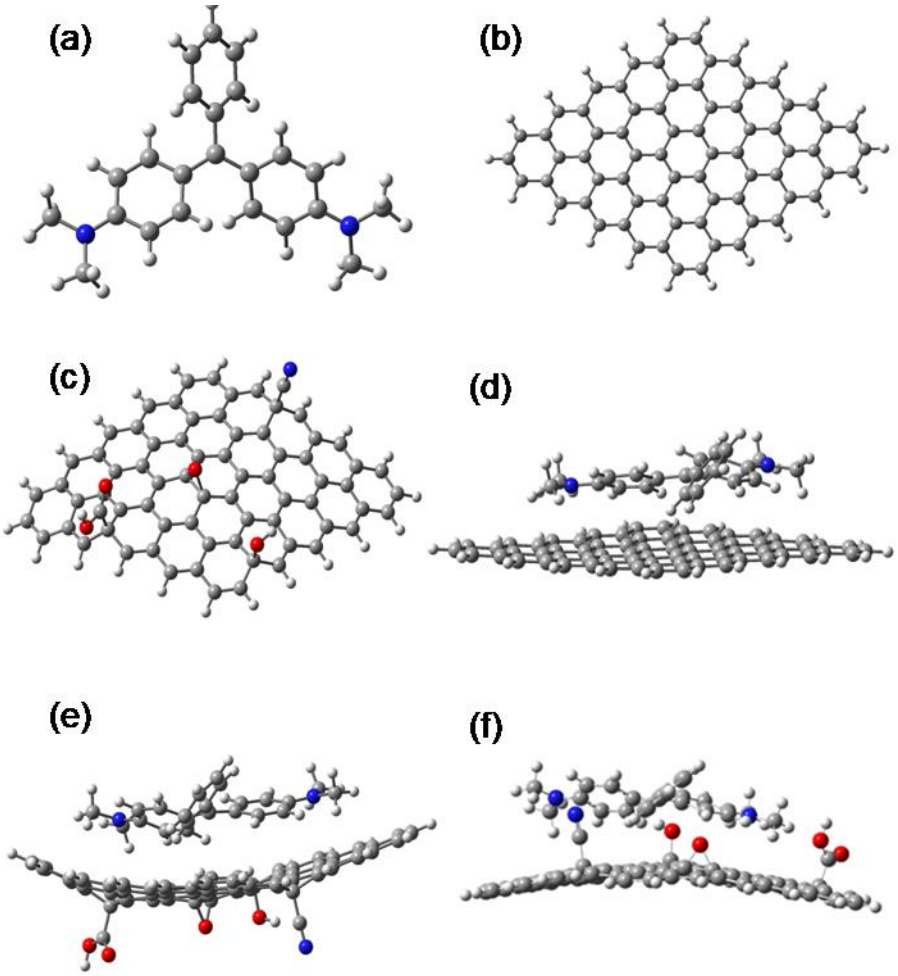

Figure 3.12: Optimized geometries of (A) Malachite green, (B) model of carbon quantum dot, (C) functionalised model of carbon quantum dot, (D) complex of malachite green with model of carbon quantum dot and (E) complex of malachite green with graphitic face of functionalised model of carbon quantum dot obtained at M06-2X/6-31G(d,p) level of theory in aqueous media. (F) complex of malachite green with functionalised side of carbon quantum dot model obtained at M06-2X/6-31G(d,p) level of theory in aqueous media. Colour code for atoms: grey-carbon, blue-nitrogen, red-oxygen, white- hydrogen

3.2.10 Analysis of Real Aquaculture Samples for the Presence of Malachite Green

Owing to their fascinating analytical features like high sensitivity and good precision, the analytical performance of the carbon dot-based detection system was

further evaluated to detect MG in real aquaculture water samples. Water samples from two different ponds in the aquaculture fisheries of BHU, Varanasi, were collected. Samples were centrifuged at 15,000 rpm at 25°C for 15 minutes and filtered through 0.22 μ filter membrane to remove any particulate matter. Carbon dots were added to make the final concentration 35 μg/ml. The samples were spiked with different concentrations of MG (9.1-54.6 nM) and analysed by PL measurements demonstrating the potential of the present sensing system for the detection of MG in environmental samples (Figure 3.13A&B). The sensing behaviour of the carbon dots in aquaculture water samples is very similar to that of fluorescence quenching in ultrapure water. The photoluminescence spectra showed regular decrease in fluorescence intensity as seen while using ultrapure water as solvent. Hence, this method could be applied in the future for the rapid and inexpensive detection of MG in aquaculture water samples.[37,47]

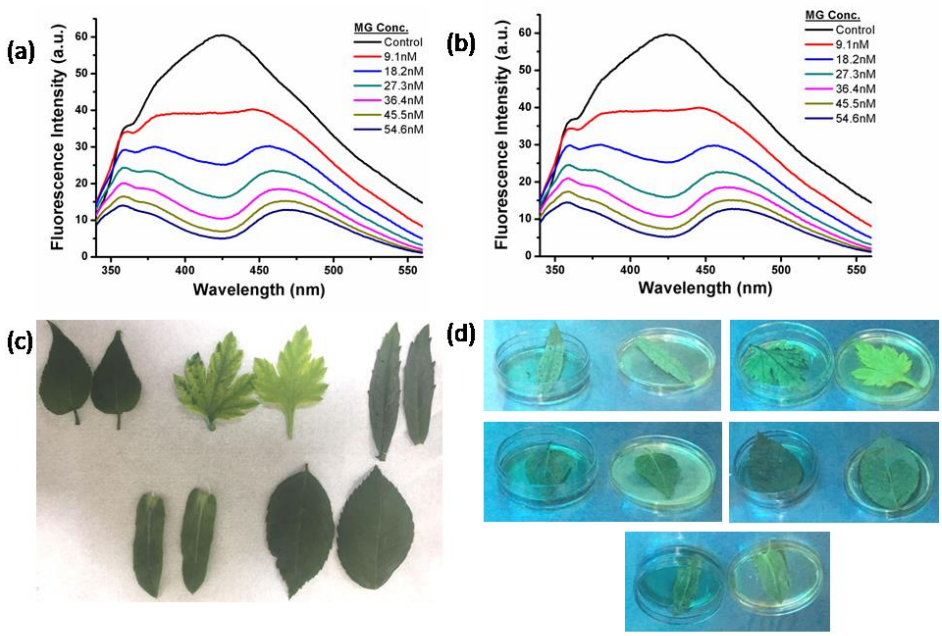

Figure 3.13: Analysis of Real Samples for Practical Toxicity Sensing in Aquaculture and Model Green Leaves. Fluorescence quenching for detection of spiked concentrations of malachite green in (A) aquaculture fisheries pond 1 sample (B) aquaculture fisheries pond 2 sample (C) sample green leaves set for all test samples (with malachite green on left) and control samples (without malachite green on right) (D) calorimetric difference seen between test and control on illuminating with UV source by fluorescence quenching

3.2.11 Analysis of Green Plant Leaves for the Detection of Malachite Green Traces by CQDs

To apply the fluorescence based detection system of carbon dots to detect trace adulterant MG residues left on vegetable material, few leaf samples were taken as test material and briefly dipped in malachite green solution having a concentration of 1 mg/ml. The leaves were air-dried and immersed in carbon dot solution followed by mild shaking. Leaves without treatment were taken as control and immersed in carbon dot solution as well. These samples were viewed under UV light to see visual difference between the two sets. Clear distinction was observed between the test leaf solution and control because of quenching of the carbon dot fluorescence and also because of the strong dark colour of malachite green itself clearly indicating that this

mechanism can be employed for devising a simple practical detection system to detect residual malachite green on green vegetables (Figure 3.13C&D).

3.2.12 Calorimetric Sensor Design

Many useful devices have been made for practical applicability of various properties.[66,67] Inspired by the result above, a simple easily-operable and portable device for households was designed for the practical detection of traces of malachite green on green vegetables used for adulteration. The design comprises a simple circuit with a switch for UV source LED light connected in series illuminating two separate chambers (Figure 3.14A). Lower chamber is completely enclosed and filled with carbon dots in solution for control while the upper chamber is also filled with the same solution in addition to a sieve which traps the vegetable test material. On shaking, the residual malachite green comes in contact with the solution leading to prominent quenching and colour change of solution increasing the calorimetric contrast between the test and control which can be viewed easily (Figure 3.14B).

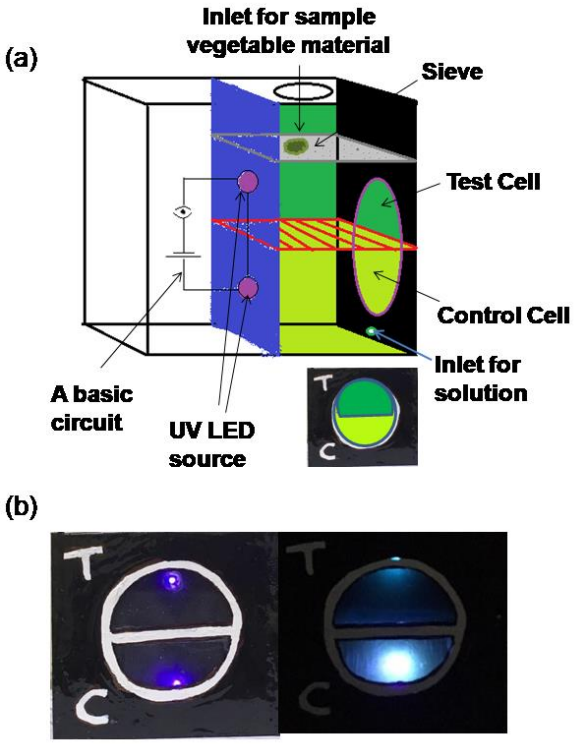

Figure 3.14: Calorimetric Sensor Design. (A) Schematic diagram of chromic sensor design for the detection of malachite green in green vegetable samples (B) Left: calorimetric sensor with empty cells having UV LED switched on; Right: calorimetric sensor with carbon quantum dot solution showing optical difference between test and control cell for the detection of malachite green

3.3 Conclusions

We have devised a simple sustainable fluorescence-based detection system for malachite green, a common food adulterant in developing and poor countries. A simple, economical, large-scalable, and eco-friendly route to synthesize hydrophilic carbon dots derived from medicinal source with a uniform size of ~3 nm through hydrothermal method was followed using *Tulsi* leaves as precursor. The prepared quantum dots show excellent properties which enable them to be used as antioxidants. They show minimal cytotoxicity in various bacterial and fungal strains. We have also shown the practical applicability of malachite green sensing in aquaculture and green vegetable adulteration testing. This strategy proved to be facile, fast and sensitive. It

had a simplistic design allowing great scope for practical use in developing countries in common households. The presented fluorescence-based method in this study would open a new avenue for the easy and rapid toxic chemical detection using carbon dot nanoprobes, by avoiding the complex modification of synthetic fluorophores via covalent bond linking between a receptor and a fluorophore. In the future, the potential of the as-prepared carbon dots would be exploited for constructing other fluorescence detection platforms and in biological applications.

3.4 References

1. Culp, S. J.; Beland F. A. Malachite Green: A Toxicological Review *Journal of the American College of Toxicology* **1996**, 15, 219-238

2. Srivastava, S.; Sinha, R.; Roy. Toxicological effects of malachite green *Aquatic Toxicology* **2004**, 66, 319–329

3. Tan, E.; Yin, P.; You, T.; Wang,H.; Guo L. Three Dimensional Design of Large-Scale TiO_2 Nanorods Scaffold Decorated by Silver Nanoparticles as SERS Sensor for Ultrasensitive Malachite Green Detection *ACS Applied Materials and Interfaces* **2012**, 4, 3432−3437

4. Mitrowska, K.; Posyniak, A.; Zmudzki J. Determination of malachite green and leucomalachite green in carp muscle by liquid chromatography with visible and fluorescence detection *Journal of Chromatography A* **2005**, 1089, 187–192

5. Huang, Y.; Ma, Y.; Hu, H.; Guo, P.; Miao, L.; Yang, Y.; Zhang, M. Rapid and sensitive detection of trace malachite green and its metabolite in aquatic products using molecularly imprinted polymer-coated wooden-tip electrospray ionization mass spectrometry *RSC Advances* **2017**, 7, 52091–52100

6. Yang, M.; Fang, J.; Kuo, T.; Wang, D.; Huang, Y.; Liu, L.; Chen, P.; Chang, T. Production of Antibodies for Selective Detection of Malachite Green and the Related Triphenylmethane Dyes in Fish and Fishpond Water *Journal of Agricultural and Food Chemistry* **2007**, 55, 8851–8856

7. Xing, W.; He, L.; Yang, H.; Sun, C.; Li, D.; Yang, X.; Li, Y.; Deng, A. Development of a sensitive and group-specific polyclonal antibody-based enzyme-linked immunosorbent assay (ELISA) for detection of malachite green and leucomalachite green in water and fish samples *J Sci Food Agric* **2009**, 89, 2165–2173

8. Lin, Z.; Zhang, H.; Li, L.; Huang, Z. Application of magnetic molecularly imprinted polymers in the detection of malachite green in fish samples *Reactive and Functional Polymers* **2016**, 98, 24 –30

9. Stead, S. L.; Ashwin, H.; Johnston, B. H.; Dallas, A.; Kazakov, S. A.; Tarbin, J. A.; Sharman, M.; Kay, J.; Keely, B. J. An RNA-Aptamer-Based Assay for the Detection and Analysis of Malachite Green and Leucomalachite Green Residues in Fish Tissue *Anal. Chem.* 2010, 82, 2652–2660

10. W. Xu, Y. Lu, Label-Free Fluorescent Aptamer Sensor Based on Regulation of Malachite Green Fluorescence Anal Chem. 2010, 82, 574–578.

11. M. Yoshizawa, K. Suzuki, A. Kubo, S. Saikan, Femtosecond study of S2 fluorescence in malachite green in solutions Chem. Phys. Lett. 1998, 290, 43–48.

12. F. Ding, L. Wei, L. Feng, Z. Li, Y. Sun, A study of the interaction between malachite green and lysozyme by steady-state fluorescence J. Fluoresc. 2009, 19, 783–791

13. Wang, Y.; Hu, A. Carbon quantum dots: synthesis, properties and applications *J. Mater. Chem. C*, **2014**, 2, 6921–6939

14. Zhu, S.; Song, Y.; Zhao, X.; Shao, J.; Zhang, J.; Yang, B. The photoluminescence mechanism in carbon dots (graphene quantum dots, carbon nanodots and polymer dots): current state and future perspective *Nano Research* **2014**, 8, 355–381

15. Zhili Peng, Z.; Han, X.; a, Li, S.; Al-Youbi, A. O.; c, Abdulaziz S. Bashammakh, A. S.; Mohammad S. El-Shahawi, M. S.; Roger M. Leblanc, R. M. Carbon dots: Biomacromolecule interaction, bioimaging and nanomedicine *Coordination Chemistry Reviews* **2017**, 343, 256–277

16. Yang, Y.; Ji, X.; Jing, M.; Hou, H.; Zhu, Y.; Fang, L.; Yang, X.; Chen, Q.; Banks, C. E. Carbon dots supported upon N-doped TiO_2 nanorods applied into sodium and lithium ion batteries *J. Mater. Chem. A* **2015**, 3, 5648-5655

17. Jiang, K.; Zhang, L.; Lu, J.; Xu, C.; Cai, C.; Lin, H. Triple-Mode Emission of Carbon Dots: Applications for Advanced Anti-Counterfeiting *Angew .Chem. Int. Ed.* **2016**, 55,7231–7235

18. Jiang, K.; Sun, S.; Zhang, L.; Lu, Y.; Wu, A.; Cai, C.; Lin, H. Red, Green, and Blue Luminescence by Carbon Dots: Full-Color Emission Tuning and Multicolor Cellular Imaging *Angew.Chem. Int. Ed.* **2015**, 54, 5360–5363

19. Wang, J.; Qiu, J. A review of carbon dots in biological applications. J Mater Sci **2016**, 51, 4728–4738

20. Qin, L. L.; Fang, L. Y.; Lei, Z.; Yue, L.; Zhi, H. C. One-step synthesis of fluorescent hydroxyls-coated carbon dots with hydrothermal reaction and its application to optical sensing of metal ions *Sci China Chem* **2011**, 54, 1342–1347

21. Castillo, A. S.; Avidad, M. A.; Pritz, C.; Robles, M. C.; Ferna´ndez, B.; Rama, M. J. R.; Ferna´ndez, A. M.; Ferna´ndez, A. L.; Gonzalez, F. S.; Fischer, A. S.; Vallvey, L. F. C. Carbon dots for copper detection with down and upconversion fluorescent properties as excitation *source Chem. Commun.* **2013**, 49, 1103-1105

22. Journet, C.; Maser, W. K.; Bernier, P.; Loiseau, A.; Chapelle, M. L.; Lefrant, S.; Deniard, P.; Leel, R.; Fischer, J. E. Large-scale production of single-walled carbon nanotubes by the electric-arc technique *Letters to Nature* **1997**, 388, 755-758

23. Li, X.; Wang, H.; Shimizu, Y.; Pyatenko, A.; Kawaguchi, K.; Koshizaki, N. Preparation of carbon quantum dots with tunable photoluminescence by rapid laser passivation in ordinary organic solvents *Chem. Commun.* **2011**, 47, 932–934

24. Panniello, A.; Mauro, A. E. D.; Fanizza, E.; Depalo, N.; Agostiano, A.; Curri, M. L.; Striccoli, M. Luminescent Oil Soluble Carbon Dots Towards White Light Emission: A Spectroscopic Study *The Journal of Physical Chemistry C* **2018**, 122, 839–849

25. Deka, M. J.; Chowdhury, D.; Chiral carbon dots and their effect on the optical properties of photosensitizers *RSC Adv.* **2017**,7, 53057–53063

26. Wang, J.; Wang, C.; Chen, Su. Amphiphilic Egg-Derived Carbon Dots: Rapid Plasma Fabrication, Pyrolysis Process, and Multicolor Printing Patterns *Angewandte Chemie* **2016**, 51, 9297-9301

27. Li, H.; He, X.; Kang, Z.; Huang, H.; Liu, Y.; Liu, J.; Lian, S.; Tsang, C. H. A.; Yang, X.; Lee, S. Water-Soluble Fluorescent Carbon Quantum Dots and Photocatalyst Design *Angew. Chem. Int. Ed.* **2010**, 49, 4430–4434

28. Wang, J.; Sahu, S.; Sonkar, S. K.; Tackett II, K. N.; Sun, K. W.; Liu, Y.; Maimaiti, H.; Anilkumar, P.; Sun, Y. Versatility with carbon dots – from overcooked BBQ to brightly fluorescent agents and photocatalysts *RSC Advances* **2013**, 3, 15604-15607

29. Wang, Q.; Huang, X.; Long, Y.; Wang, X.; Zhang, H.; Zhu, R.; Liang, L.; Teng, P.; Zheng, H. Hollow luminescent carbon dots for drug delivery *Carbon* **2013**, 59, 192-199

30. Ding, H.; Yu, S. B.; Wei, Ji. S.; Xiong, H. M. Full-Color Light-Emitting Carbon Dots with a Surface-State-Controlled Luminescence Mechanism *ACS Nano* **2016**, 10, 484−491

31. Mehta, V. N.; Jha, S.; Basu, H.; Singhal, R. K.; Kailasa, S. K.; One-step hydrothermal approach to fabricate carbon dots from apple juice for imaging of mycobacterium and fungal cells *Sensors and Actuators B* **2015**, 213, 434–443

32. De, B.; Karak, N. A green and facile approach for the synthesis of water soluble fluorescent carbon dots from banana juice *RSC Advances* **2013**, 3, 8286-8290

33. Liu, Y.; Liu, Y.; Park, M.; Park, S.; Zhang, Y.; Akanda, M. R.; Park, B.; Kim, H. Y. Green synthesis of fluorescent carbon dots from carrot juice for in vitro cellular imaging *Carbon Letters* **2017**, 21, 61-67

34. Zhao, S.; Lan, M.; Zhu, X.; Xue, H.; Ng, T.; Meng, X.; Lee, C.; Wang, P.; Zhang, W. Green Synthesis of Bifunctional Fluorescent Carbon Dots from Garlic for Cellular

Imaging and Free Radicals Scavenging *ACS Applied Materials & Interfaces* **2015**, 7, 17054–17060

35. Li, C.; Ou, C.; Huang, C.; Wu, W.; Chen, Y.; Lin, T.; Ho, L.; Wang, C.; Shih, C.; Zhou, H.; Lee, Y.; Tzeng, W.; Chiou, T.; Chu, S.; Cang, J.; Chang, H. Carbon dots prepared from ginger exhibiting efficient inhibition of human hepatocellular carcinoma cells *J. Mater. Chem. B*, **2014**, 2, 4564 –4571

36. Li, L.; Wang, X.; Fu, Z.; Cui, F. One-step hydrothermal synthesis of nitrogen- and sulfur-co-doped carbon dots from ginkgo leaves and application in biology *Materials Letters* **2017**, 196, 300–303

37. Liu, R.; Zhang, J.; Gao, M.; Li, Z.; Chen, J.; Wu, D.; Liu, P. A facile microwave-hydrothermal approach towards highly photoluminescent carbon dots from goose feathers *RSC Adv.* **2015**, 5, 4428-4433

38. Liu, S.; Wang, C.; Li, C.; Wang, J.; Mao, L.; Chen, S; Hair-derived carbon dots toward versatile multidimensional fluorescent materials *J. Mater. Chem. C* **2014**, 2, 6477–6483

39. Sahu, S.; Behera, B.; Maiti, T. K.; Mohapatra, S. Simple one-step synthesis of highly luminescent carbon dots from orange juice: application as excellent bio-imaging agents *Chem. Commun* .**2012**, 48, 8835–8837

40. Wang, N.; Wang, Y.; Guo, T.; Yang, T.; Chen, M.; Wang, J. Green preparation of carbon dots with papaya as carbon source for effective fluorescent sensing of Iron (III) and *Escherichia coli Biosensors and Bioelectronics* **2016**, 85, 68–75

41. Essner, J. B.; Laber, C. H.; Ravula, S.; Polo-Parada, L.; Baker, G. A. Pee-dots: biocompatible fluorescent carbon dots derived from the upcycling of urine *Green Chem.* **2016**, 18, 243

42. Pires, N. R.; Santos, C. M. W.; Sousa, R. R.; de Paula, R. C. M.; Cunha, P. L. R.; Feitosa, P. A. Novel and Fast Microwave-Assisted Synthesis of Carbon Quantum Dots from Raw Cashew Gum *J. Braz. Chem. Soc.* **2015**, 26, 1274-1282

43. Huang, G.; Chen, X.; Wang, C.; Zheng, H.; Huang, Z.; Chen, D.; Xie, H. Photoluminescent carbon dots derived from sugarcane molasses: synthesis, properties, and applications *RSC Adv.* **2017**, 7, 47840–47847

44. Miao, H.; Wang, L.; Zhuo, Y.; Zhou, Z.; Yang, X. Label-free fluorimetric detection of CEA using carbon dots derived from tomato juice *Biosensors and Bioelectronics* **2016**, 86, 83–89

45. Zhou, J.; Sheng, Z.; Han.; Zou, M.; Li, C. Facile synthesis of fluorescent carbon dots using watermelon peel as a carbon source *Materials Letters* **2012**, 66, 222–224

46. Verma, S. Chemical constituents and pharmacological action of *Ocimum sanctum* (Indian holy basil-Tulsi) *The Journal of Phytopharmacology* **2016**, 5, 205-207

47. Kumar, A.; Chowdhuri, A. R.; Laha, D.; Mahto, T. K.; Karmakar, P.; Sahu, S. K. Green synthesis of carbon dots from Ocimum sanctum for effective fluorescent sensing of Pb^{2+} ions and live cell imaging *Sensors and Actuators B* **2017**, 242, 679–686

48. Tan, M.; Zhang, L.; Tang, R.; Song, X.; Li, Y.; Wu, H.; Wang, Y.; Lv, G.; Liu, W.; Ma, X.; Enhanced photoluminescence and characterization of multicolour carbon dots using plant soot as a carbon source *Talanta* **2013**, 115, 950–956

49. Zhang, Q.; Zhang, C.; Li, Z.; Ge, J.; Li, C.; Dong, C.; Shuang, S. Nitrogen-doped carbon dots as fluorescent probe for detection of curcumin based on the inner filter effect *RSC Adv.* **2015**, 5, 95054–95060

50. Wang, Z.; Liao, H.; Wu, H.; Wang, B.; Zhao, H.; Tan, M. Fluorescent carbon dots from beer for breast cancer cell imaging and drug delivery *Anal. Methods* **2015**, 7, 8911–8917

51. Liang, Q.; Ma, W.; Shi, Y.; Li, Z.; Yang, X. Easy synthesis of highly fluorescent carbon quantum dots from gelatin and their luminescent properties and applications *Carbon* **2013**, 60, 421-428

52. Pandey, S.; Thakur, M.; Mewada, A.; Anjarlekar, D.; Mishra, Sharon, M. Carbon dots functionalized gold nanorod mediated delivery of doxorubicin: tri-functional

nano-worms for drug delivery, photothermal therapy and bioimaging *J. Mater. Chem. B* **2013**, 1, 4972–4982

53. Zhao, L.; Di, F.; Wang, D.; Guo, L.; Yang, Y.; Wan, B.; Zhang, H. Chemiluminescence of carbon dots under strong alkaline solutions: a novel insight into carbon dot optical properties **2013**, 5, 2655–2658

54. Mitra, S.; Chandra, S.; Kundu, T.; Banerjee, R.; Pramanik, P.; Goswami, A. Rapid microwave synthesis of fluorescent hydrophobic carbon dots *RSC Advances*, **2012**, **2**, 12129-12131

55. Dehghani, A.; Ardekani, S. M.; Hassan, M.; Gomes, V. G. Collagen derived carbon quantum dots for cell imaging in 3D scaffolds via two-photon spectroscopy *Carbon* **2018**, 131, 238-245

56. Anilkumar, P.; Wang, X.; Cao, Li.; Sahu, S.; Liu, J.; Wang, P.; Korch, K.; Tackett II, K. N.; Parenzan, A.; Sun, Y. Toward quantitatively fluorescent carbon-based ‘‘quantum’’ dots *Nanoscale* **2011**, 3, 2023–2027

57. Barman, M. K.; Jana, B.; Bhattacharyya, S.; Patra, A. Photophysical Properties of Doped Carbon Dots (N, P, and B) and Their Influence on Electron/Hole Transfer in Carbon Dots−Nickel (II) Phthalocyanine Conjugates *J. Phys. Chem. C*, 118, 20034−20041

58. Wang, X.; Cao, L.; Lu, F.; Meziani, M. J.; Li, H.; Qi, G.; Zhou, B.; Harruff, B. A.; Kermarrec, F.; Sun, Y. Photoinduced electron transfers with carbon dots *Chem Commun (Camb)*. **2009**, 25, 3774–3776

59. Du, F.; Zhang, M.; Li, X.; Li, J.; Jiang, X.; Li, Z.; Hua, Y.; Shao, G.; Jin, J.; Shao, Q.; Zhou, M.; Gong, A. Economical and green synthesis of bagasse derived fluorescent carbon dots for biomedical applications *Nanotechnology* **2014**, 25

60. Wang, H.; Sun, C.; Chen, X.; Zhang, Y.; Colvin, V. L.; Rice, Q.; Seo, J.; Feng, S.; Wang, S.; Yu, W. W. Excitation wavelength independent visible color emission of carbon dots *Nanoscale* **2017**, 9, 1909-1915

61. Zhang, R.; Liu, Y.; Yu, L.; Li, Z.; Sun, S. Preparation of high-quality biocompatible carbon dots by extraction, with new thoughts on the luminescence mechanisms *Nanotechnology* **2013**, 24

62. Liu, Z. X.; Chen, B. B.; Liu, M. L.; Zou, H. Y.; Huang, C. Z. Cu(I)-Doped carbon quantum dots with zigzag edge structures for highly efficient catalysis of azide–alkyne cycloadditions *Green Chem.* **2017**,19, 1494–1498

63. Khan, S.; Gupta, A.; Verma, N. C.; Nandi, C. K. Time-Resolved Emission Reveals Ensemble of Emissive States as the Origin of Multicolor Fluorescence in Carbon Dots *Nano Letters* **2015**, 15, 8300–8305

64. Christensen, I. L.; Sun, Y.; Juzenas, P. Carbon Dots as Antioxidants and Prooxidants *Journal of Biomedical Nanotechnology* **2011**, 7, 667–676

65. Zhang, Q. Q.; Chen, B. B.; Zou, H. Y.; Li, Y. F.; Huang, C. Z. Inner filter with carbon quantum dots: A selective sensing platform for detection of hematin in human red cells *Biosensors and Biomolecules* **2018**, 100, 148-154

66. Gao, Q.; Han, J.; Ma, Z. Polyamidoamine dendrimers-capped carbon dots/Au nanocrystal nanocomposites and its application for electrochemical immunosensor *Biosensors and Bioelectronics* **2013**, 49, 323–328

67. Li, C.; Adamcik, J.; Mezzenga, R. Biodegradable nanocomposites of amyloid fibrils and graphene with shape-memory and enzyme-sensing properties *Nature Nanotechnology*, **2012**, 7, 421-427